An Advanced PV Simulation Model for Electric Vehicles with Photovoltaic Installations

Christian Schuss*, Bernd Eichberger†, and Tapio Fabritius*
*Optoelectronics and Measurement Techniques (OPEM) Research Unit, University of Oulu, Finland;
email: christian.schuss, tapio.fabritius@oulu.fi
†Institute of Electronic Sensor Systems, Graz University of Technology, Austria; email: bernd.eichberger@tugraz.at

***Abstract*—In this paper, we investigate the difference between charging electric vehicles with photovoltaic (PV) installations installed on top of buildings and PV installations embedded into vehicles. In future, photovoltaics will be integrated into hybrid electric vehicles (HEVs), battery-powered electric vehicles (BEVs) as well as into connected and autonomous vehicles (CAVs) for extending the electrical driving range (EDR) of these types of vehicles. Over the past decade, charging patterns of electric vehicles have been studied extensively and how the costs for electricity affect the time for charging electric vehicles. If PV cells are embedded for example into the roof of an electric vehicle, electricity can be produced wherever the car goes, both, under parking and driving conditions. We discuss how these circumstances will affect and change the calculation of charging patterns for electric vehicles.**

***Index Terms*—battery-powered electric vehicle, data acquisition, environmental data, hybrid electric vehicle, measurement, photovoltaic energy, simulation, solar energy.**

I. Introduction

Hybrid electric vehicles (HEVs), battery-powered electric vehicles (BEVs) as well as connected and autonomous vehicles (CAVs) have lead to a strong increase in electricity demand of the individual transportation sector [1], [2]. With the increase in number of passenger vehicles worldwide over the forthcoming years [3], it can be said the the electricity demand of the passenger vehicles will increase as well [1], [2]. Even though these types of vehicles can help to reduce emissions within urban areas, it is worth noting that at present the required electricity for HEVs, BEVs, and CAVs is mainly produced by non-renewable energy resources such as coal, oil, gas and nuclear power (COGN) [4], [5]. Charging too many electric vehicles at the same time represents challenges to the power grid [2].

In order to overcome these challenges, researchers have proposed to utilise solar energy within charging stations for electric vehicles [6]. Doing so helps to stabilise the power grid on one hand and allows to reduce carbon dioxide emissions on the other [6], [7]. Solar energy is also used for prolonging the lifetime of battery-powered Internet of Things (IoT) devices. By embedding photovoltaic (PV) cells into these types of electronic devices, energy can be harvested for charging the devices' batteries from the surrounding environment [8]. Likewise, PV cells can be integrated into electric vehicles to produce solar energy, both, under parking and driving conditions [9]–[12].

Araki *et al.* estimate that by integrating PV cells into passenger vehicles, about 70% of the required electricity by the vehicle can be produced by the vehicle's own PV installation [13]. However, in order to achieve this high percentage level, the specific conditions for integrating PV cells into passenger vehicles need to be well understood. For example, the amount of irradiation on top of vehicle differs to the available irradiation on the roof of a building [14]. As a result, some surface areas of an electric vehicle are more suitable for PV energy production than others. In addition, a large number of PV cells can be needed as seen on the recent prototype of Toyota which 1,188 PV cells in order to provide the HEV with sufficient electrical energy [15].

Forecasting and estimating the potential PV energy of the vehicle's PV installation is important. Doing so allows to provide drivers with vital information about the possible extension of the electrical driving range (EDR) of their cars [13]. Similarly, forecasts can help to stabilise the power grid [2]. Commonly, PV simulation models are used for calculating the potential output power of flat PV panels on the roof of buildings [16], [17]. However, as a result of the different circumstances of the PV installation on top of an electric vehicle, in particular the curved shape of the vehicle's roof and partial shading effects, the conventional simulation model needs to be modified [14], [18].

In this work, we present an advanced PV simulation model which takes into account the given circumstances for PV installations on top of curved surfaces such as the roof or the bonnet of an electric vehicle. As PV cells will be aligned under different angles towards the sun, their irradiation and PV cell temperature will be different as well. Since in a conventional PV model it is assumed that each PV cell receives the exact same solar radiation level and operates at the exact same PV cell temperature, the conventional PV model is not suitable of precisely calculating or estimating the potential output power of PV installation on top of electric vehicles.

For the verificiation of the simulation results and to calculate the parameters of the advanced PV simulation model, we built two experimental structures that allowed us to measure and analyse the performance of PV cells under different alignments towards the sun. The measurement results from these experiments were used for the development of the advanced PV simulation model. In this paper, we present the simulation results and illustrate how the PV installation integrated in the

roof an electric vehicle on the example of the Toyota Prius can be calculated for an entire day. The model also takes into account the different orientation of the car itself towards the sun.

II. Simulation and Experimental Results

A. Measurement of the Impact of Ambient Conditions

In this work, two experimental structures were built to compare the simulated results with measurement results. Fig. 1 shows the first structure, which was used to measure the available output power of a single PV cell. The orientation of the PV cell was alternated by a servo motor controlled by an Arduino microcontroller which also stored the data to a microSD-card. The alignment of the PV cell towards the sun was changed on a continous basis by one degree. One cycle consisted of 125 ° (*i.e.* 90 ° to -45 °) resulting in 125 measurements. A real-time clock module was used to provide a timestamp for the measurement data.

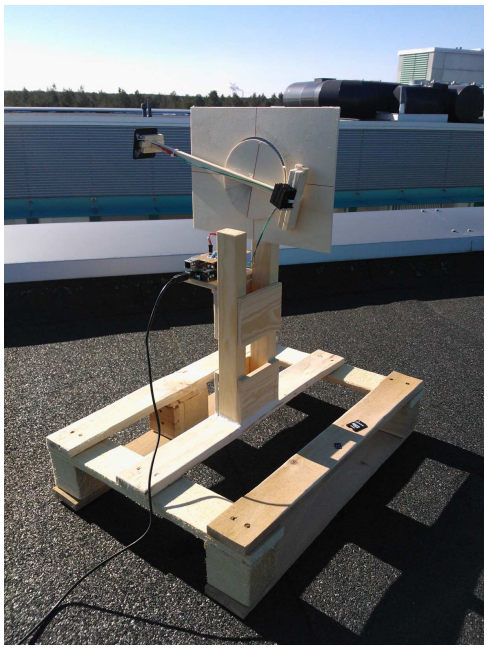

Fig. 1: Experimental structure 1 for measuring photovoltaics

B. Measurement of the Impact of Interconnections

Fig. 2 show the second structure on which the PV cells were aligned under the same angle as on the top of the Toyota Prius. Similar to the rows of PV cells on vehicle's roof, the structure allowed to measure one or several PV cells under the same angle at a given time. PV cells were connected with each other to measure the impact of the different alignment of PV cells over a longer period of time. Likewise, the impact of different connections between PV cells at different angles on the potential output power of PV cells was investigated [9], [19]. The obtained information from both structures was used to verify the paramters in the simulation model with the help of the Newton-Raphson algorithm.

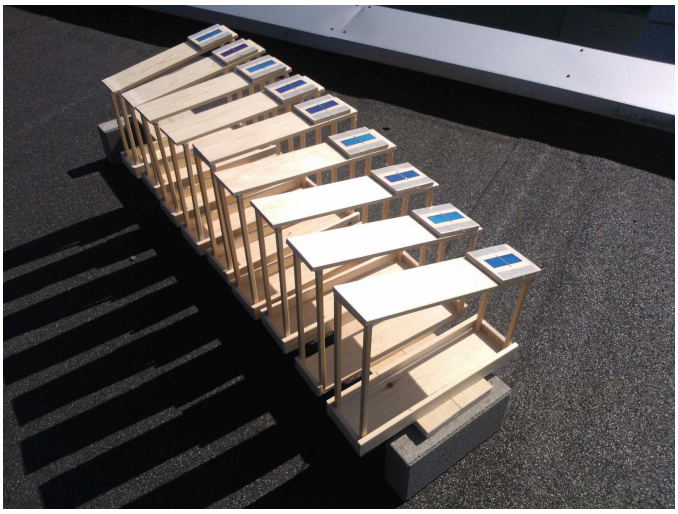

Fig. 2: Experimental structure 2 for measuring photovoltaics

III. Simulation of Photovoltaics

A. Purpose of Simulating Photovoltaics

Simulations are helpful for determining the potential output power of photovoltaics under different solar radiation levels (λ) and PV cell temperature levels (T_c). In this section, we present a PV simulation model suitable for calculating the output power of PV cells embedded into electric vehicles. Generally speaking, PV simulation models are required to compute the Current-Voltage (*I-V*) and Power-Voltage (*P-V*) curves under different ambient conditions. In this way, we can get a better understanding of PV cells as power source on top of electric vehicles such as BEVs, HEVs and CAVs. Furthermore, the potential PV energy can be estimated which can be used either for charging the electric vehicle's high-voltage battery during standstill or prolonging the electric driving range (EDR) during operation.

A single PV cell provides a certain level of voltage (V) and current (I). For example, we can connect two PV cells in series to double the possible output voltage. Hence, we include two factors into the simulation to model different interconnections of PV cells. On one hand, this is the factor for the cells connected in series (N_s) and, on the other hand, cells connected in parallel (N_p). For a single PV cell, N_s and N_p are equal to 1. In PV simulation models, different interconnections do not change the shape of the *I-V* curve, but the scale of the x-axis (*i.e.* in the case of a series connection) or y-axis (*i.e.* in the case of parallel connection). However, in practice, this simplification is not valid due to individual differences within PV cells and tolerance limits provided by PV manufacturers.

B. Conventional and Advanced PV Simulation Model

Commonly, the single diode model is used as an equivalent electric circuit for the simulation of one PV cell [8], [16], [19], [20]. In the literature, depending on the available information and required accuracy of the model, different types of PV simulation models are used. Parameters for simulation models

such as the open-circuit voltage (V_{oc}) and the short-circuit current (I_{sc}) can be obtained from the PV manufacturer's datasheet. In addition, some parameters such as the ideality factor (A) can be estimated with typical values for the respective PV cell material to simplify simulations. For a higher degree of accuracy, parameter identification techniques are used to calculate more suitable values for parameters [16].

1) Ideal Model: The ideal model allows a simulation with only a few parameters. Hence, the accuracy compared to data sets (voltage/current records under different solar radiation and temperature levels) can be limited. First, we assume the PV cell as a current source, which creates a photocurrent (I_{ph}) in direct proportion to given solar radiation level (λ), and a diode, as shown in Fig. 3. The output current (I_{out}) is restricted by the diode current (I_d). We obtain the output current (I_{out}) as

$$I_{out} = I_{ph} - I_d \tag{1}$$

which is, with the Shockley diode equation:

$$I_{out} = I_{ph} - I_s(e^{\frac{qV_{out}}{AkT_c}} - 1) \tag{2}$$

where I_s is the saturation current, q is the charge of an electron, V_{out} is the output voltage, k is Bolzmann's constant, and A is the ideality factor of the p-n junction. The photocurrent (I_{ph}) is calculated by

$$I_{ph} = I_{sc,ref}(1 + K_I(T_c - T_{ref}))\frac{\lambda}{\lambda_{ref}} \tag{3}$$

where $I_{sc,ref}$ is the short-circuit current at reference conditions, K_I is the temperature coefficient for current, T_{ref} is the PV cell temperature at reference conditions, and λ_{ref} is the solar radiation level at reference conditions. Furthermore, the saturation current (I_s) of the cell is obtained by

$$I_s = I_{rs}(\frac{T_c}{T_{ref}})^3 e^{qE_g(\frac{1}{T_{ref}} - \frac{1}{T_c})} \tag{4}$$

where I_{rs} is the reverse saturation current and E_g is the band gap energy of the seminconductor. The reverse saturation current (I_{rs}) is calculated by

$$I_{rs} = \frac{I_{sc}}{e^{\frac{qV_{oc,ref}(1+K_V(T_c - T_{ref}))}{AkT_c}} - 1} \tag{5}$$

where $V_{oc,ref}$ is the open-circuit voltage of the cell at reference conditions and K_V is the temperature coefficient for voltage.

2) Simplified Model: For a higher degree of accuracy, a series resistance (R_s) is included into the equivalent circuit considering the PV cell's internal resistance, in particular the current path through the semiconductor, the contacts, the metal grid and current collecting bus. This parameter can vary through different applications of PV cells. The loss of the series resistance (R_s) is considered in Equation (2) as

$$I_{out} = I_{ph} - I_s(e^{\frac{q(V_{out} + I_{out}R_s)}{AkT_c}} - 1) \tag{6}$$

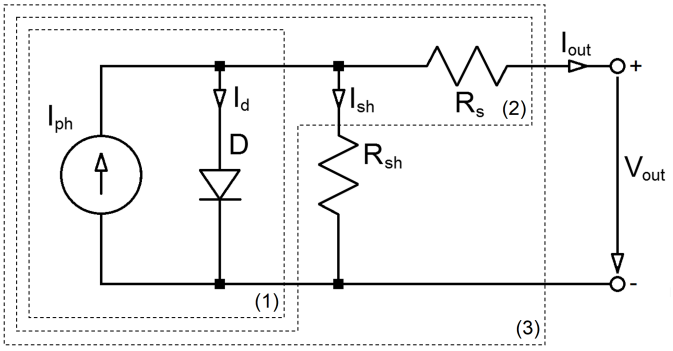

Fig. 3: Schematic of the PV simulation models

3) Practical Model: For silicon-based PV cells, the practical model offers an excellent degree of accuracy. A shunt resistance (R_{sh}) is included into the equivalent circuit taken into account the leakage current of the PV cell. Due to the shunt resistance (R_{sh}), Equation (6) is extended to

$$I_{out} = I_{ph} - I_s(e^{\frac{q(V_{out} + I_{out}R_s)}{AkT_c}} - 1) - \frac{V_{out} + I_{out}R_s}{R_{sh}} \tag{7}$$

It is worth noting that parameters such as $V_{oc,ref}$, $I_{sc,ref}$, T_{ref}, λ_{ref}, K_V, K_I, N_s, and N_p can be obtained from the data sheet and specifications of PV manufacturers.

4) Advanced Model: Generally speaking, PV cells can be connected in series and/or parallel with each other to form a PV panel. Usually, PV panels are made out of a large series connection of PV cells [9], [13], [16], [17], [19]. Furthermore, in conventional PV simulation models, one coefficient is applied for each, the solar radiation level (λ) and the PV cell temperature (T_c). In other words, the assumption is made that each cell of a PV panel is exposed to an equal amount of sunlight and operates at the exact same temperature level. Thus, Equation (7) is modified into

$$I_{out} = N_p I_{ph} - N_p I_s(e^{\frac{q(N_p V_{out} + N_s I_{out} R_S)}{N_p N_s AkT_c}} - 1) - \frac{\frac{N_p}{N_s}V_{out} + I_{out}R_s}{R_{sh}} \tag{8}$$

However, this assumption can be made in the case of conventional PV panels which are mounted onto flat surfaces, for example on the roof of a building. If PV cells are embedded into the roof of an electric vehicle, PV cells are aligned under different longitudinal angles and, thus, receive different amounts of irradiation and operate at different temperatures. For this reason, PV cells which are either installed or embedded on top of curved surfaces such as the roof of an electric vehicle, an advanced model must be used which allows to simulate each PV cell which different parameters. As a result, the conventional model for a PV panel, shown in Fig 4 must be modified in order to allow the simulation of PV cells installed on top of curved surfaces.

As PV cells are exposed to different solar radiation levels on top of curved surfaces, they will operate at different PV

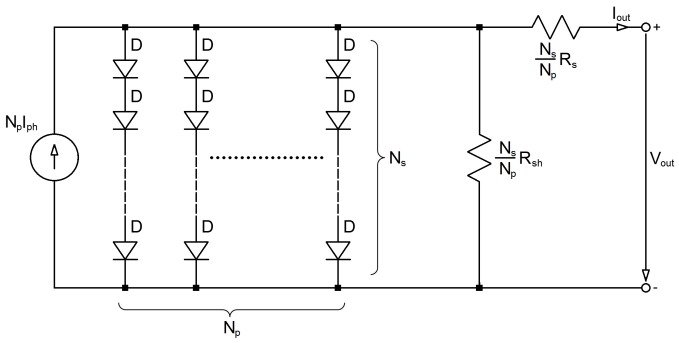

Fig. 4: Common model: Equivalent circuit of a PV panel

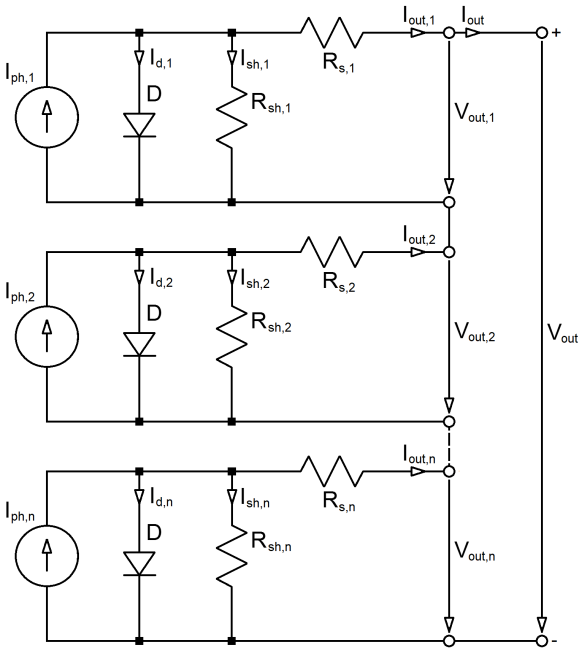

Fig. 5: Advanced model: Equivalent circuit of a PV panel

temperature levels. Furthermore, they will produce different levels of output current levels. These circumstances must be considered in the PV simulation model. Hence, the equivalent circuit, shown in Fig. 4, needs to be modified to allow simulating PV cells with different solar radiation levels. Fig. 5 presents the equivalent circuit of a PV panel in the output current of each PV cell (I_{out}) is calculated individually. When forming series connections of PV cells, the output current is determined by the weakest PV cell of the interconnection, in other words, the PV cell with the lowest solar radiation level [19], [20], calculated as follows

$$\begin{aligned} I_{out} &= \min\{I_{out,i}\} \quad i = 1, 2, \ldots, n \\ &= \min\{I_{ph,i} - I_{s,i}(e^{\frac{q(V_{out,i}+I_{out,i}R_{s,i})}{AkT_{c,i}}} - 1) \\ &\quad - \frac{V_{out,i} + I_{out,i}R_{s,i}}{R_{sh,i}}\} \end{aligned} \tag{9}$$

while the output voltage (V_{out}) is the sum of the individual

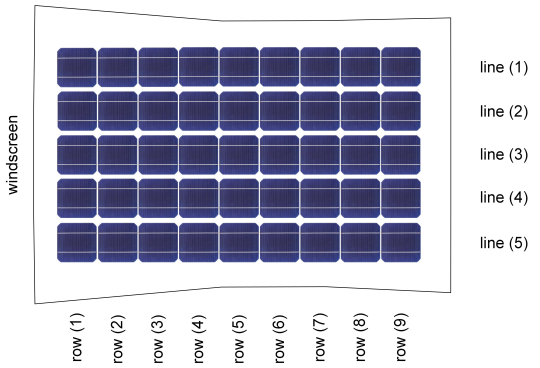

Fig. 6: PV installation on top of the Toyota Prius

output voltages of PV cells, obtained as follows

$$V_{out} = \sum_{i=1}^{n} V_{out,i} \tag{10}$$

IV. Photvoltaics on Top of Curved Surfaces

A. Longitudinal Angles of PV cells

When embedding PV cells into curved surfaces such as the roof of electric vehicles, each PV cell will be aligned under a different longitudinal angle (β) towards the sun. Fig. 6 illustrates the PV installation on top of the experimental vehicle, a Toyota Prius [9]. As a result of the curved shape of the roof of the Toyota Prius, the five PV cells in each row have a different orientation towards the sun. Table I summarises the given β of the PV cells from row number (1) to (9). As shown in Fig. 6, conventional silicon-based PV cells with a size of 156x156 millimetres were used for the PV installation. However, as in [15], also smaller PV cells can be used to optimise and maximise the use of the available area on top of an electric vehicle.

B. Estimating the Irradiation on Top of Curved Surfaces

In practice, measuring the solar radiation level for each PV cell with a certain longitudinal angle and, thereby, obtaining information on the available irradiation on top of each PV cell is not possible. Hence, a method has to be found which allows to estimate the solar radiation level based on the irradiation obtained on a horizontal level (β = 0 °). Based on these longitudinal angles, there is a difference in the orientation of 24 ° between the PV cells in row number (1) and row number (9). Fig. 7 presents the available solar radiation level (λ) and PV cell temperature (T_c) for the 15th of June in the City of Oulu, Finland [20]. The angle of the solar altitude (α) and solar azimuth (θ) are shown in Fig. 8. Usually, θ = 180 ° at noon, however, daylight saving time (DST) in June causes a shift by one hour.

In [21], we introduced the concept of the effective area (A_{eff}) of a PV cell. A_{eff} was calculated in MATLAB® by using the perpendicular area without taking diffuse irradiation and possible total reflections into account. In this research, we extend the concept of A_{eff} for the consideration of the solar

TABLE I: Longitudial angles of PV cells (β) on the roof of the Toyota Prius

row (1)	row (2)	row (3)	row (4)	row (5)	row (6)	row (7)	row (8)	row (9)
15 °	12 °	9 °	3 °	2 °	0 °	– 3 °	– 7 °	– 9 °

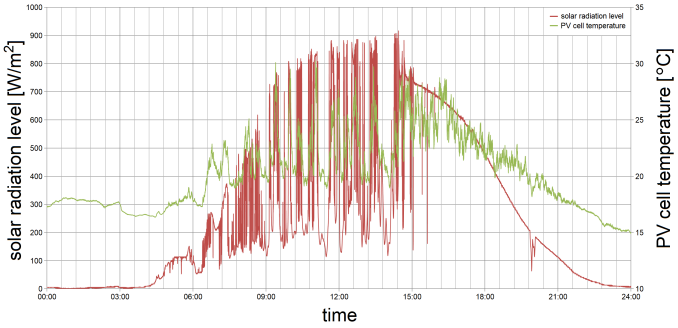

Fig. 7: λ and T_c for the whole day

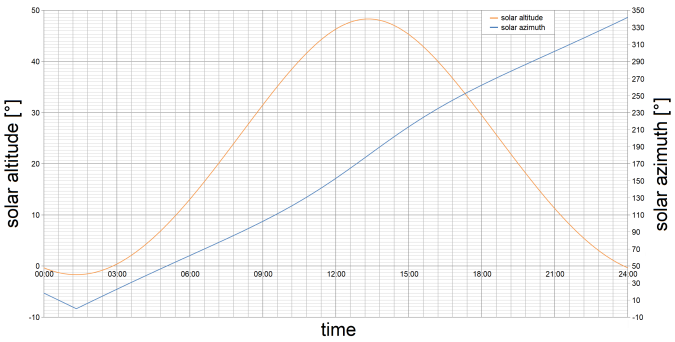

Fig. 8: α and θ for the whole day

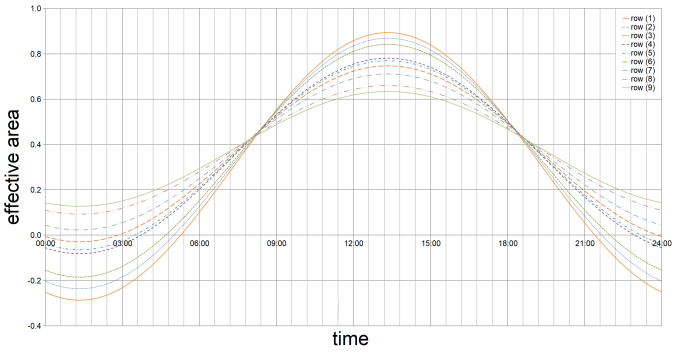

Fig. 9: Effective area for ψ = 180 °

azimuth angle (θ) and the cardinal direction of the vehicle's orientation (ψ) as follows

$$A_{eff} = cos(\alpha)sin(\beta)cos(\psi - \theta) + sin(\alpha)cos(\beta) \qquad (11)$$

Figs. 9 and 10 illustrate A_{eff} for ψ = 180 ° (*i.e.* vehicle's front orientated towards the south) and for ψ = 0 ° (*i.e.* vehicle's front orientated towards the north), respectively. As in the case of PV installations on the roof of houses, it is advisable to orientate the PV installation on top of a vehicle towards the south. However, as seen in Fig. 9, due to the non-linear curved

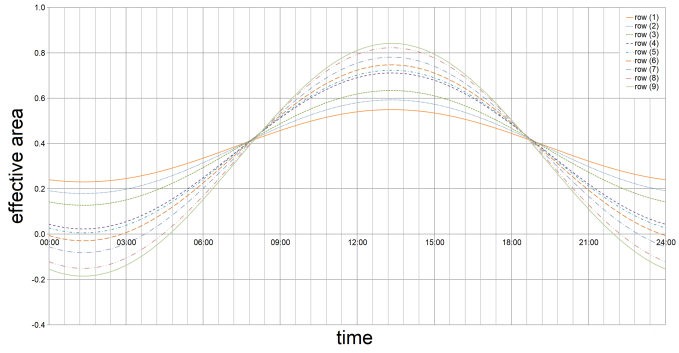

Fig. 10: Effective area for ψ = 0 °

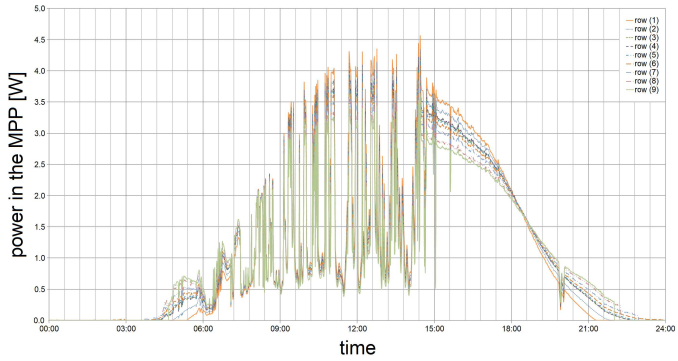

Fig. 11: Power in the MPP for ψ = 180 °

shape of the roof, this type of orientation brings more sunlight to the front rows, *e.g.* row (1) and row (2), and less sunlight to the rows in the back, *e.g.* row (8) and row (9). Similar to [21], the obtained values for A_{eff} are normalised against row (6), as follows

$$\hat{A}_{eff,i} = \frac{A_{eff,i}}{A_{eff,6}} \quad \text{whereas} \quad i = 1, 2, \ldots, 8, 9 \qquad (12)$$

Then, from the data on the amount of irradiation available in row (6), the solar radiation level in other rows (λ_i) is estimated.

$$\lambda_i = A_{eff,i} \times \lambda \quad \text{whereas} \quad i = 1, 2, \ldots, 8, 9 \qquad (13)$$

In experiments, we verfied the impact of different longitudinal angles and, thus, different solar radiation levels on the PV cell temperature. We found out that a change in λ of 1 W/m^2 causes a change in T_c of about 0.1 °C. This correlation was used in the PV simulation model to estimate the PV cell temperature in other rows ($T_{c,i}$) based on the PV cell temperature obtained in row (6).

Fig. 11 shows the simulation results, in other words the calculated power in the MPP (P_{mpp}) for ψ = 180 °. At 06:00, θ = 62.32 ° and, as seen in Fig. 12, the sun is located behind the car in the east north east (ENE). Hence, as seen in Fig.

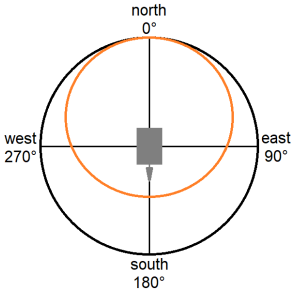

Fig. 12: θ vs. ψ = 180 °

11, more power is obtained from the PV cells in the rear of the car. At noon, θ = 152.88 ° the sun is in the south south east (SSE) and, thus, the highest amount of power is obtained from the PV cells in the front of the car. At 18:00, the sun is in the west at θ = 271.4 °. As seen in Fig. 12, at 18:00, the sun transitions from being in front of the vehicle towards being behind the vehicle. This transition can also be seen in Fig. 11. Again, as in the morning, more power can be obtained from the PV cells in the rear than in the front of the car.

V. Conclusion

In this paper, we presented an advanced PV simulation model that allows calculating the potential output power of PV installations on top of HEVs, BEVs, and CAVs. In conventional PV simulation models, it is assumed that each PV cell of a panel receives the same amount of irradiation and operates at the exact same temperature level. However, this assumption can be made for flat PV panels installed on top of buildings, but not for electric vehicles due to the curved shape of the roof. Hence, each PV cell in each row of the installation needs to be simulated individually.

In addition, the vehicle's orientation has to be taken into account. In our analyses, we elaborated how the vehicle's orientation towards the sun either increases or decreases the individual output power of PV cells depending on their longitudinal angle. As a result, the overall output power in the MPP is affected based on the parking orientation of the vehicle. In our simulation model, we used real environmental data to calculate the output power of the experimental vehicle's PV installation. In future work, we would like to analyse the circumstances including the energy requirments of different types of HEVs, BEVs, and CAVs to provide more detailed estimations on the possible extension of the EDR.

Acknowledgment

Dr. Christian Schuss was funded by the SMAD project, which is part of the Academy of Finland 6Genesis (6G) project (grant no. 318927). Prof. Tapio Fabritius is partially supported by Academy of Finlands FIRI funding (grant no. 320017).

References

[1] M. Taiebat, A.L. Brown, H.R. Safford, S. Qu, and M. Xu, "A review on energy, environmental, and sustainability implications of connected and automated vehicles, *Environmental science & technology*, vol. 52, no. 20, pp. 11449-11465, 2018.

[2] N. Canter, "How will the growing use of plug-in electric vehicles affect the power grid?, *TLT*, vol. 74, no. 4, pp. 12-13, 2018.

[3] Number of passenger cars and commercial vehicles in use worldwide from 2006 to 2015 in (1,000 units) https://www.statista.com/statistics/281134/number-of-vehicles-in-use-worldwide/ [accessed 16 September 2019], 2018.

[4] D.P. van Vuuren, N. Nakicenovic, K. Riahi, A. Brew-Hammond, D. Kammen, V. Modi, and K. Smith, "An energy vision: The transformation towards sustainability - interconnected challenges and solutions", *Current Opinion in Environmental Sustainability*, vol. 4, issue: 1, pp. 18-34, 2012.

[5] S. Mekhilef, R. Saidur, and A. Safari, "A review on solar energy use in industries", *Renewable and Sustainable Energy Reviews*, vol. 15, issue: 4, pp. 1777-1790, 2011.

[6] G.R.C. Mouli, P. Bauer, and M. Zeman, "System design for a solar-powered electric vehicle charging station for workplaces, *Applied Energy*, vol. 168, pp. 434-443, 2016.

[7] Today in Energy. EIA projects world energy consumption will increase 56% by 2040. Vol. July. Available https://www.eia.gov/todayinenergy/detail.cfm?Id=12251‡ [accessed 16 September 2019], 2013.

[8] L. Cai, N. Dai, and Z. Tan, "Research on mathematical model and calculation simulation of wireless sensor solar cells in Internet of Things, *Journal Wireless Communication Networks*, vol. 1, p. 116, 2018.

[9] C. Schuss, T. Fabritius, B. Eichberger, and T. Rahkonen, "Moving Photovoltaic Installations: Impacts of the Sampling Rate on Maximum Power Point Tracking Algorithms, *IEEE Transactions on Instrumentation and Measurement*, vol. 68, no. 5, pp. 1485-1493, 2019.

[10] D. P. Birnie, III, "Analysis of energy capture by vehicle solar roofs in conjunction with workplace plug-in charging, *Solar Energy*, vol. 125, pp. 219-226, 2016.

[11] C. Schuss, T. Kotikumpu, B. Eichberger, and T. Rahkonen, "Impact of Dynamic Environmental Conditions on the Output Behaviour of Photovoltaics, *20th IMEKO TC4 International Symposium and 18th International Workshop on ADC Modelling and Testing*, pp. 993-998, 2014.

[12] T.L. Gibson and N.A. Kelly, "Solar photovoltaic charging of lithium-ion batteries, *Proceedings of the IEEE Vehicle Power Propulsions Conference*, pp. 310-316, 2009.

[13] K. Araki, L. Ji, G. Kelly, and M. Yamaguchi, "To Do List for Research and Development and International Standardization to Achieve the Goal of Running a Majority of Electric Vehicles on Solar Energy", *Coatings*, vol. 8, issue: 7, pp. 251, 2018.

[14] Y. Ota, T. Masuda, K. Araki, and M. Yamaguchi, "A mobile multi-pyranometer array for the assessment of solar irradiance incident on a photovoltaic-powered vehicle", *Solar Energy*, vol. 184, pp. 84-90, 2019.

[15] Toyota Is Testing a New Solar-Powered Prius by D. Grossman https://www.popularmechanics.com/cars/hybrid-electric/a28322554/toyota-is-testing-a-new-solar-powered-prius/ [accessed 20 November 2019], 2019.

[16] H.-L. Tsai, "Insolation-oriented model of photovoltaic module using Matlab/Simulink", *Solar Energy*, vol. 84, issue 7, pp. 1318-1326, 2010.

[17] M.G. Villalva, J.R. Gazoli, and E.R. Filho, "Comprehensive Approach to Modeling and Simulation of Photovoltaic Arrays", *IEEE Transactions on Power Electronics*, vol. 24, no. 5, pp. 1198-1208, 2009.

[18] K. Araki, K.H. Lee, T. Masuda, Y. Hayakawa, N. Yamada, Y. Ota, and M. Yamaguchi, "Rough and Straightforward Estimation of the Mismatching Loss by Partial Shading of the PV Modules Installed on an Urban Area or Car-Roof", *IEEE 46th Photovoltaic Specialists Conference (PVSC)*, pp. 1218-1225, 2019.

[19] C. Schuss, H. Gall, K. Eberhart, H. Illko, and B. Eichberger, "Alignment and Interconnection of Photovoltaics on Electric and Hybrid Electric Vehicles", *Proceedings of the IEEE International Instrumentation and Measurement Technology Conference (I2MTC)*, pp. 524-527, 2014.

[20] C. Schuss, B. Eichberger, and T. Rahkonen, "Impact of Sampling Interval on the Accuracy of Estimating the Amount of Solar Energy", *Proceedings of the IEEE International Instrumentation and Measurement Technology Conference (I2MTC)*, pp. 1355-1360, 2016.

[21] C. Schuss, B. Eichberger, and T. Rahkonen, "Calculating the Output Power of Photovoltaic Cells on Top of Electric and Hybrid Electric Vehicles", *Proceedings of the IEEE International Instrumentation and Measurement Technology Conference (I2MTC)*, pp. 820-825, 2019.